

# Poly(thieno[3,4-*b*]thiophene): A p- and n-Dopable Polythiophene Exhibiting High Optical Transparency in the Semiconducting State

Gregory A. Sotzing\* and Kyunghoon Lee

Department of Chemistry and the Polymer Program, Institute of Materials Science, University of Connecticut, Storrs, Connecticut 06269-3136

Received March 11, 2002

**ABSTRACT:** Herein we report the synthesis and electrochemical characterization of poly(thieno[3,4-*b*]thiophene), a new low band gap conducting polymer with a high redox switching stability that exhibits high optical transparency in the semiconductive state. The monomer, thieno[3,4-*b*]thiophene (T34bT), has a low oxidation potential for polymerization, 1.02 V vs Ag/Ag<sup>+</sup> (1.25 V vs SCE), a potential between that for the oxidation of 3,4-ethylenedioxythiophene and pyrrole. Poly(T34bT) has a band gap of ca. 0.85 eV (1459 nm) as determined by the onset for the  $\pi$ -to- $\pi^*$  transition from the UV-vis-NIR spectrum and 0.8 V from the difference in the onsets for both the p- and n-doping processes from cyclic voltammetry. Stability studies as determined from chronocoulometry and chronoabsorptometry indicate that the polymer retains 95% electroactivity and 96% change in optical density after 100 double potential steps. Poly-(T34bT) is sky-blue in the reduced form and optically transparent (no observable color) in the oxidized state with a coloration efficiency of 160 cm<sup>2</sup>/C at 800 nm.

## Introduction

Industrial and academic interest has continued to heighten in intrinsically conductive polymers (ICP) ever since their discovery approximately 25 years ago.<sup>1</sup> This is particularly due to limited understanding of such systems and their potential broad applicability in numerous macro- and nanoscale electronic devices. Presently, commercially viable applications utilizing conductive polymers include charge dissipation films,<sup>2</sup> light-emitting diodes (LED),<sup>3</sup> electrochromic displays,<sup>4</sup> and their use as volatile organic gas sensors.<sup>5</sup> Furthermore, a present area of heightened interest is their potential use as molecular (nanometer sized) wires.<sup>6</sup>

Another target application for ICPs is the replacement of indium-doped tin oxide coatings as optically transparent electrodes. The present state-of-the-art ICP being explored and utilized as a transparent conductor is poly-(3,4-ethylenedioxythiophene), also known as PEDOT or Baytron-P.<sup>7</sup> The monomer, 3,4-ethylenedioxythiophene, has a low peak oxidation potential of ca. 1.35 V vs the saturated calomel electrode<sup>8</sup> and is readily suspended and polymerized in water utilizing chemical oxidation agents.<sup>9</sup> PEDOT is sky-blue in the conducting state with electrical conductivities reported as high as 80 S/cm for PEDOT films cast from aqueous solution.<sup>10</sup> PEDOT has a relatively low band gap ( $E_g$ ) of 1.7 eV with respect to poly(thiophene), which has an  $E_g$  of 2.1 eV.<sup>11</sup> Despite this relatively low  $E_g$ , upon oxidation, there is a tail for the absorption attributed to the higher  $\pi$ -to-bipolaron transition extending into the longer wavelengths of the visible spectrum which is responsible for the observed sky-blue color of the polymer in the semiconducting state.<sup>11</sup>

The band structure of conducting polymers dictates their electrochemical and optical properties. The band structure can be tuned by altering either or both the electronic structure and sterics of the backbone.<sup>12</sup> Of particular interest is the preparation of stable, low band gap conductive polymers. These materials have at-

tracted much attention due to their high visible transmissivity in the conductive form and their ease at which they can be both p- and n-doped. The first low band gap ( $E_g$ ) polymer reported was poly(isothianaphthene) ( $E_g$  = ca. 1.0–1.2 eV),<sup>13</sup> making the band gap approximately 1 eV lower than that of polythiophene. This has been attributed to the ability of the fused benzene ring to stabilize the quinoidal form of the polymer in the conductive state. Despite this, the practical use of poly-(isothianaphthene) is limited due to its environmental instability.<sup>13</sup>

Previously, we have communicated our preliminary work on the electrochemical polymerization and characterization of a low band gap intrinsically conducting polymer consisting of the thieno[3,4-*b*]thiophene repeat unit.<sup>14</sup> Herein, we report a more complete study of the electrochemistry and optical properties of this system, extending the fundamental electrochemical analysis to the potential application of this material to electrochromic displays and windows.

## Experimental Section

**Materials.** 3,4-Dibromothiophene was used as received (Lancaster Synthesis Inc.) or prepared in accordance with literature procedure starting from thiophene.<sup>15</sup> Bis(triphenylphosphino)palladium(II) chloride, copper(I) iodide, triphenylphosphine, sulfur, *n*-butyllithium (*n*-BuLi) in hexanes, sodium hydride, lithium trifluoromethanesulfonate, and tetrabutylammonium hexafluorophosphate were used as received from Aldrich. Before use, the molarity of *n*-butyllithium in hexanes was determined via titration using 1,10-phenanthroline (Aldrich) in accordance to literature.<sup>16</sup> Diethylamine (ACROS Organics) was distilled over potassium hydroxide before use. Acetonitrile (Fisher Scientific) was used after distillation over calcium hydride. Tetrabutylammonium perchlorate (TBAP) was prepared via addition of perchloric acid to an aqueous solution of tetrabutylammonium bromide followed by filtration, recrystallization from ethanol, and drying under vacuum. It should be noted that proper precautions should be taken when using perchloric acid. 3-Bromo-4-(trimethylsilyl)ethynylthiophene was prepared and purified in accordance to the literature procedure.<sup>17</sup>

**Instrumentation.** Nuclear magnetic resonance (NMR) spectra were obtained using either a Bruker 500 MHz or a

\* Corresponding author. e-mail sotzing@mail.ims.uconn.edu.

Bruker 400 MHz spectrometer, mass spectra were obtained using a Hewlett-Packard 5890 series II gas chromatography/mass spectrometer (GC/MS), and Fourier transform infrared spectroscopy (FTIR) was performed using a MAGNA-IR 560.  $^1\text{H}$  NMR data are reported as follows: chemical shift (multiplicity: d = doublet, dd = doublet of doublets; integration value;  $J$  value in hertz; peak assignment).  $^1\text{H}$  and  $^{13}\text{C}$  chemical shifts are reported in ppm downfield from tetramethylsilane (TMS) reference using the residual protonated solvent resonance as an internal standard. A CH instruments 660A potentiostat was used for all electrochemistry experiments. Polymer film thicknesses were measured on electrode-supported films with a Tencor Instruments Alpha Step 200 profilometer. Optoelectrochemistry was obtained with the aid of a Perkin-Elmer Lambda 900 UV/vis/NIR spectrometer.

**Synthesis of the Thieno[3,4-*b*]thiophene.** All equipment was vacuum-dried and argon-purged before use. A 1000 mL round-bottom, three-necked flask equipped with a thermometer was charged with 450 mL of dry diethyl ether and 34.4 g (133 mmol) of 3-bromo-4-(trimethylsilyl)ethynylthiophene while under argon. This solution was maintained at a temperature of  $-78\text{ }^\circ\text{C}$  and stirred for an additional 30 min, after which 58.6 mL of *n*-BuLi (2.4 M in hexanes, 141 mmol) was slowly added dropwise via a syringe over a period of 1 h while keeping the temperature of the solution below  $-75\text{ }^\circ\text{C}$ . After addition, the solution was stirred for 2 h at  $-78\text{ }^\circ\text{C}$ , and then the solution was allowed to warm to ca.  $-45\text{ }^\circ\text{C}$ , which took approximately 1 h to achieve. The reaction mixture was allowed to stir for an additional hour while maintaining a temperature of  $-45\text{ }^\circ\text{C}$ . Sulfur (4.54 g, 141 mmol) was then added slowly over a 10 min period to the flask via a solids addition funnel, and the reaction mixture was allowed to warm to ca.  $-35\text{ }^\circ\text{C}$  in order to fully dissolve the sulfur. After approximately 10 min the initially cloudy solution that resulted immediately after sulfur addition had changed to clear yellow. The reaction mixture was then cooled to  $-45\text{ }^\circ\text{C}$ , and stirring was continued for an additional 2 h. Then the reaction mixture was slowly warmed to  $-10\text{ }^\circ\text{C}$  over a period of 30 min, and 250 mL of the reaction mixture was then added to a 500 mL separatory funnel equipped with a cooling jacket containing a brine/ice mixture held at  $-5\text{ }^\circ\text{C}$ . It should be noted that the separatory funnel was first charged with 200 mL of brine, and then this solution was cooled to  $-5\text{ }^\circ\text{C}$  before the extraction. During the extraction the aqueous layer turned cloudy yellow after 30 s. It is pertinent at this stage to separate the layers. After the first brine wash, the same process was then repeated for the second portion (250 mL) of the reaction mixture with a fresh brine solution (200 mL). The brine layers were then combined and placed into a single-neck 1000 mL round-bottom flask under argon, and then this solution was heated to  $70\text{ }^\circ\text{C}$  and stirred for 1 h at this temperature. After cooling to room temperature, the product was extracted with ether ( $4 \times 300\text{ mL}$ ), and then the ether layers were combined, dried over  $\text{MgSO}_4$  and evaporated under vacuum. The crude product (12.8 g) was purified using vacuum distillation with an 11.3 g (61%) thieno[3,4-*b*]thiophene fraction being collected from  $38$  to  $45\text{ }^\circ\text{C}$  at 0.05 Torr as a colorless liquid.

The structure and purity were verified using gas chromatography/mass spectrometry (GC/MS), Fourier transform infrared spectroscopy and nuclear magnetic resonance spectroscopy (NMR). FTIR:  $3098$  and  $3068\text{ cm}^{-1}$  (aromatic C–H stretching),  $1489$  and  $1543\text{ cm}^{-1}$  (aromatic C=C stretching),  $759\text{ cm}^{-1}$  (C–S–C stretch),  $671\text{ cm}^{-1}$  (ring deformation). NMR:  $^1\text{H}$ ,  $^{13}\text{C}$ , COSY (correlation spectroscopy), HETCOR (heteronuclear correlation), and HMBC (heteronuclear multiple-bond connectivities) were performed in order to verify structure and to make proton and carbon peak assignments.  $^1\text{H}$  NMR  $\delta$  ( $\text{CDCl}_3$ ): 7.36 (d; 1H;  $J$  5.4 Hz, H-2), 6.94 (dd; 1H;  $J$  5.6 and 0.5 Hz; H-3), 7.26 (dd; 1H;  $J$  2.6 and 0.7 Hz; H-4), 7.35 (d; 1H;  $J$  3.1 Hz; H-6).  $^{13}\text{C}$  NMR  $\delta$  ( $\text{CDCl}_3$ ): 132.4 (C-2'), 116.8 (C-3'), 110.6 (C-4'), 111.6 (C-6'), 139.3 (C-7'), 147.6 (C-8'). It should be noted that the assignments for protons H-4 and H-6 described herein are different from those previously reported by Wynberg.<sup>18</sup> GC/MS: One observable peak in the gas chromatogram with a molecular ion at  $m/z = 140$ .

**Electrochemistry.** Either a platinum (2 mm diameter), gold (2 mm diameter), or vitreous carbon (3 mm diameter) button working electrode and platinum flag ( $1\text{ cm}^2$ ) counter electrode were used for cyclic voltammetry and for double potential step chronocoulometry experiments using button electrodes. A  $\text{Ag}/\text{Ag}^+$  nonaqueous reference electrode was employed which consisted of a silver wire immersed into a 0.01 M  $\text{AgNO}_3/0.1\text{ M}$  tetrabutylammonium perchlorate/acetonitrile solution in a glass tube fitted with a Vycor tip. The reference electrode was calibrated to be 0.47 V vs the normal hydrogen electrode (NHE) using a ferrocene standard. 0.1 M tetrabutylammonium perchlorate (TBAP)/acetonitrile, 0.1 M lithium triflate/acetonitrile, or 0.1 M tetrabutylammonium hexafluorophosphate ( $\text{TBAPF}_6$ )/acetonitrile was used as the electrolytic medium for performing electrochemical polymerizations and characterizations. For *n*-doping electrochemistry, lithium hydride was added to the electrolyte solution for the removal of water.

**Optoelectrochemical Measurement.** Poly(T34bT) films were prepared via cyclovoltammetric growth from 0.01 M T34bT in 0.1 M TBAP/acetonitrile by scanning the potential between  $-1.1$  and  $1.2\text{ V}$  for 40 cycles at a scan rate of  $100\text{ mV/s}$  using ITO-coated glass as the working electrode. After polymerization, the poly(T34bT) films were washed with acetonitrile and then placed into a glass cuvette with monomer-free electrolyte. The reference electrode was a  $\text{Ag}/\text{Ag}^+$  nonaqueous reference as described in the electrochemistry section, and the counter electrode was a platinum flag with a  $1\text{ cm} \times 0.2\text{ cm}$  hole which allows for the passage of light. All optoelectrochemical experiments were carried out under a nitrogen atmosphere.

**Electrochromics and Redox Switching Stability.** Poly-(T34bT) films were prepared via cyclovoltammetric growth from 0.01 M T34bT in 0.1 M lithium triflate/acetonitrile by scanning the potential between  $-0.75$  and  $1.2\text{ V}$  for 40 cycles at a scan rate of  $100\text{ mV/s}$  using ITO-coated glass as the working electrode. The poly(T34bT) film was then washed with acetonitrile and placed into a quartz cuvette containing 0.1 M lithium trifluoromethanesulfonate. The reference and counter electrodes were  $\text{Ag}/\text{Ag}^+$  and a platinum plate with a  $1\text{ cm} \times 0.2\text{ cm}$  hole. Chronocoulometry and chronoabsorptometry were obtained simultaneously while switching the potential between  $0.15$  and  $-0.8\text{ V}$  with 8 s pulses. Chronoabsorptometry was monitored at a wavelength of  $800\text{ nm}$ .

Chronocoulometric experiments were also carried out using a platinum button in both 0.1 M TBAP/acetonitrile and 0.1 M lithium triflate/acetonitrile. Films of poly(T34bT) for these studies were obtained via constant potential polymerization at  $1.1\text{ V}$  vs  $\text{Ag}/\text{Ag}^+$ , and films were ca.  $0.05\text{ }\mu\text{m}$  thick. All of these experiments were performed under a nitrogen atmosphere.

## Results and Discussion

**Monomer Synthesis and Characterization.** The synthesis of thieno[3,4-*b*]thiophene (T34bT) from 3,4-dibromothiophene was carried out in a manner similar to literature procedure.<sup>17,19</sup> The first step involved palladium-catalyzed coupling of 3,4-dibromothiophene with trimethylsilylacetylene in accordance with the procedure reported by Brandsma<sup>17</sup> in order to produce 3-bromo-4-(trimethylsilyl)ethynylthiophene. We have reported herein a detailed procedure for the heterocyclic ring closure of 3-bromo-4-(trimethylsilyl)ethynylthiophene to T34bT, which has been modified with respect to that originally reported<sup>19</sup> since we were unable to produce purified yields at the stated level. For example, the maximum yield that we could obtain for the ring closure utilizing the identical method to that previously reported was 8%. The ring closure to T34bT (Figure 1) involved three steps without isolation of intermediates. First, lithium halogen exchange was carried out via addition of *n*-butyllithium and was

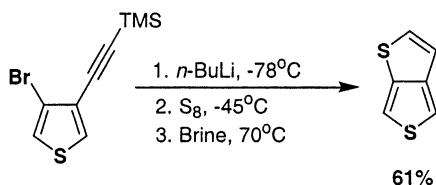


**Figure 1.** Synthesis of thieno[3,4-*b*]thiophene (T34bT) from 3-bromo-4-(trimethylsilyl)ethynylthiophene.

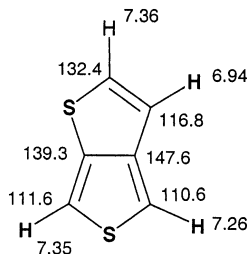


**Figure 2.**  $^1\text{H}$  and  $^{13}\text{C}$  peak assignments for T34bT reported in parts per million (ppm) from tetramethylsilane.

followed by the warming of the reaction mixture and addition of sulfur in order to produce the thiolate. The reaction was then cooled and further reacted, allowing for completion of thiolate formation. After warming to approximately  $-10^\circ\text{C}$ , an extraction with brine cooled to  $-5^\circ\text{C}$  was carried out. Of paramount importance is the separation of the aqueous layer from the organic layer. After separation, the brine layer is heated to  $70^\circ\text{C}$ , which after extraction and purification via vacuum distillation results in a 61% yield of T34bT. Thus, the overall purified yield obtained for T34bT starting from commercially available 3,4-dibromothiophene is 51%.

Although the proton nuclear magnetic resonance (NMR) peak assignments had been previously reported in the literature,<sup>18</sup> the carbon peak assignments had not been made, thereby leading us to a more comprehensive study. Figure 2 gives the proton and carbon peak assignments for T34bT utilizing  $^1\text{H}$ ,  $^{13}\text{C}$ , COSY (correlation spectroscopy), HETCOR (heteronuclear correlation), and HMBC (heteronuclear multiple-bond connectivity) nuclear magnetic resonance (NMR) spectroscopy experiments. It should be noted that from our work we have established that the peak assignments previously reported<sup>18</sup> for protons on carbon positions 2 and 6 of T34bT were incorrectly made as indicated from our HETCOR results in which the hydrogen that we have labeled as H-4 in Figure 2 shows a correlation to the carbon at  $\delta$  147.6 and the hydrogen that we have labeled as H-6 shows a correlation to the carbon at  $\delta$  139.3. Gas chromatography/mass spectrometry and Fourier transform infrared spectroscopy were also performed on T34bT for structural confirmation.

**Poly[thieno(3,4-*b*)thiophene], Poly(T34bT): Electrochemical Synthesis and Characterization.** PolyT34bT was prepared via electrochemical polymerization. Figure 3 shows the cyclic voltammetric polymerization of T34bT onto a vitreous carbon working electrode utilizing a standard three-electrode electrochemical cell. Of particular importance to this set of cyclic voltammograms is that on the first scan oxidation of the monomer occurs with an onset potential of ca. 0.8 V with a peak at 1.02 V. Therefore, oxidation of T34bT is higher than that for pyrrole, and the peak for T34bT oxidation is 0.1 V lower than that for 3,4-ethylenedioxythiophene.<sup>8</sup> At a potential above 0.8 V, T34bT undergoes electrochemical oxidation and cou-

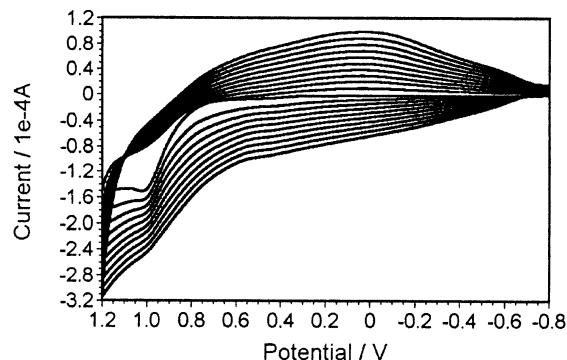


**Figure 3.** Cyclic voltammetric polymerization, 10 scans, of T34bT (0.01 M) in 0.1 M TBAP/acetonitrile electrolyte solution at a scan rate of 100 mV/s using a vitreous carbon working electrode. Potential reported vs  $\text{Ag}/\text{Ag}^+$  reference electrode (0.47 V vs NHE).

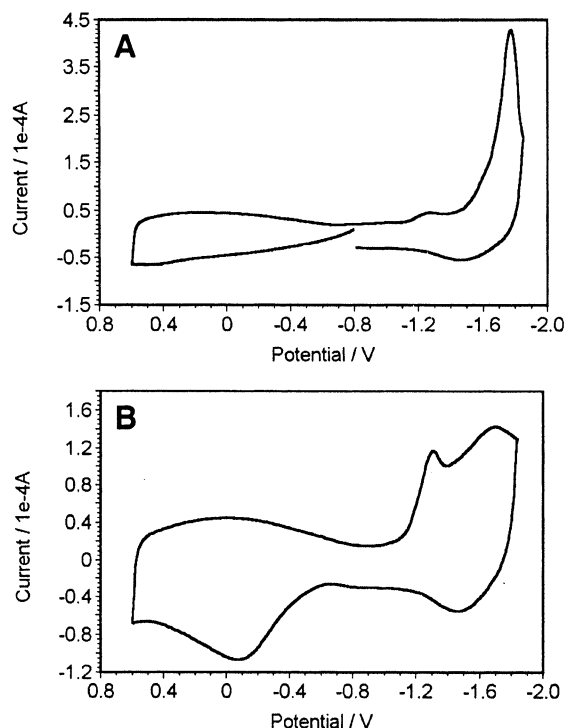
pling to produce insoluble poly(T34bT) in the intrinsically conducting form on the surface of the working electrode. Upon scan reversal, the reduction of oxidized poly(T34bT) is broad with a current maximum occurring at a potential of 0.03 V. The oxidation process of poly(T34bT) is then observed with an onset of ca.  $-0.4$  V, a lower potential than that for the oxidation of the monomer, indicating that there is more extensive conjugation of the generated insoluble electroactive species coated on the working electrode. Upon further cycling, polymerization is indicated by the increase in current response for the polymer redox process.

After polymerization, the poly(T34bT)-coated electrode was washed with acetonitrile, and the cyclic voltammetry of the polymer was obtained in electrolyte solution without monomer present. Of particular importance is that the current for the peak process for both the oxidation and reduction of the polymer is linearly proportional to the scan rate, indicating that the polymer is in direct contact to the electrode surface. Furthermore, from inspection of the cyclic voltammograms poly(T34bT) was found to have an onset for oxidation at ca.  $-0.6$  V with a peak at ca. 0.4 V. These potentials are approximately equivalent to the potentials reported for the oxidation of poly(3,4-ethylenedioxythiophene) and for poly(pyrrole).<sup>20</sup>

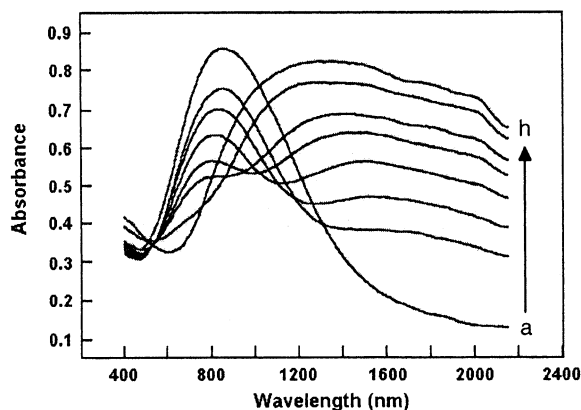
In addition to using the TBAP/acetonitrile electrolyte and vitreous carbon working electrode, we have utilized tetrabutylammonium hexafluorophosphate ( $\text{TBAPF}_6$ )/acetonitrile, ( $\text{TBABF}_4$ )/acetonitrile, and lithium triflate/acetonitrile electrolytes and both platinum and gold working electrodes. Despite the electrolyte solution and the working electrodes that were studied, the electrochemical polymerizations and electrochemical redox processes of the poly(T34bT)s obtained therefrom were found to be nearly identical with only slight shifts,  $<0.05$  V, in the monomer and polymer oxidation peak potentials.

Figure 4 shows the first two scans of 30 total scans for the cyclic voltammetry of poly(T34bT) from  $-1.85$  to 0.6 V in 0.1 M TBAP/acetonitrile. Within this CV the polymer is taken through both the oxidation, hole injection, and the reduction, electron injection, of the neutral polymer. The cyclic voltammogram (Figure 4A) was initiated at a potential of  $-0.8$  V and is scanned in the positive direction. At  $-0.6$  V the onset for oxidation of the polymer occurs with a small maximum for the oxidation process occurring at ca. 0.4 V. Upon potential reversal at 0.6 V and further scanning in the cathodic





**Figure 4.** p- and n-doping cyclic voltammetry of poly(T34bT) on a vitreous carbon working electrode at a scan rate of 100 mV/s in 0.1 M TBAP/acetonitrile showing the first scan (A) and the second scan (B).



**Figure 5.** UV-vis-NIR spectrum of a 0.1  $\mu\text{m}$  thick poly(thieno[3,4-*b*]thiophene) film on ITO glass at different potentials. The film was first electrochemically reduced at  $-0.8$  V, dipped into a 0.1 M TBAP/acetonitrile containing 0.2 vol % hydrazine for full reduction, and then placed into a 0.1 M TBAP/acetonitrile, and the UV-vis-NIR spectrum was taken (a). Poly(T34bT) was then sequentially oxidized to (b)  $-0.4$ , (c)  $-0.3$ , (d)  $-0.2$ , (e)  $-0.1$ , (f)  $0.0$ , (g)  $0.15$ , and (h)  $0.4$  V vs Ag/Ag<sup>+</sup> reference electrode ( $0.47$  V vs NHE).

direction, the peak for the reduction of the oxidized polymer occurs at ca. 0 V. Upon further scanning in the cathodic direction, a reductive process occurs with an onset of  $-1.5$  V and a peak at  $-1.7$  V. This has been commonly attributed to the injection of electrons or n-doping of the neutral conjugated polymer. Upon polarity reversal at  $-1.85$  V and scanning in the anodic direction, the peak for the oxidation of the n-doped polymer is evident at  $-1.5$  V. Figure 5B shows the second scan carried out for this polymer through both the p- and n-doping processes. The major difference between the first (Figure 4A) and second scan (Figure 4B) is that the oxidation process of neutral poly(T34bT)

occurs at a substantially lower potential of  $-0.08$  V, ca. 0.5 V lower than that for the oxidation of the polymer in the first scan, and that the peak for the oxidation process becomes more pronounced. This is quite different than the results for other low band gap polymers. For example, typically after going through the n-doping process, the p-doping process will have a sharp onset peak before the main oxidation process of the polymer<sup>12</sup> attributed to the existence of trapped charged states (electrons) within the polymer.<sup>21</sup> Poly(T34bT) shows this behavior before the n-doping at a potential of  $-1.3$  V which could be attributed to trapped holes in the polymer; however, it does not show this behavior for the oxidation process of the polymer after n-doping since there is only one broad peak centered at ca. 0 V.

The n-doping of poly(T34bT) is quite stable to redox cycling. For example, upon cycling the polymer 30 times through the n-doped form after the second scan, there is only a loss of 20% electroactivity. This stability is relatively high compared to the limited number of n-dopable conjugated polymers that have been previously reported.<sup>12</sup> From the difference of the onsets for both the p- and n-doping processes, the band gap ( $E_g$ ) of poly(T34bT) as determined from cyclic voltammetry (Figure 4B) is calculated to be approximately 0.8 V.

**Optoelectrochemistry.** A ca. 0.12  $\mu\text{m}$  thick film of poly(T34bT) was prepared via electrochemical polymerization onto an indium-doped tin oxide (ITO)-coated glass slide. The polymer was then reduced at  $-0.8$  V and dipped into 0.1 M TBAP/acetonitrile containing 0.2 vol % hydrazine, and the UV-vis-NIR spectrum (Figure 5, trace a) of the film was obtained. The  $E_g$  as measured by the onset for the valence to conduction band occurs at 0.85 eV (1459 nm) with a peak at 1.46 eV (846 nm), qualifying this material as a low band gap polymer.<sup>12</sup> This value is in agreement with the values of 1.54 and 1.63 eV for the aromatic and quinoidal forms, respectively, as calculated by Hong and Marynick.<sup>22</sup> Upon sequentially oxidizing the T34bT film, UV-vis-NIR spectra were obtained. As shown in Figure 5, the absorbance for the valence to conduction transition decreases upon electrochemical oxidation, and the observance of a lower energy transition for a conduction to bipolaron transition becomes apparent at  $-0.4$  V and continues to increase in intensity at ca. 1 eV (1240 nm). Furthermore, it is apparent that the tail of the absorption for the conduction to bipolaron transition continues to increase in energy upon oxidation as indicated by the shift in the isosbestic point from ca. 1300 nm for the spectra obtained at  $-0.8$  and  $-0.4$  V to 750 nm for the spectra obtained at  $-0.8$  and  $-0.4$  V as a function of oxidation potential. Nonetheless, the valence to bipolaron transition predominately remains within the NIR region of the spectrum, making this polymer uncolored and highly transparent to the naked eye. This is illustrated in Figure 6, which shows a 0.8  $\mu\text{m}$  thick film of poly(T34bT) after application of  $-0.8$  V to place it in the fully reduced state (Figure 6A) and after applying a potential of 0.4 V to put it in the fully oxidized conductive form (Figure 6B). Because of the high optical transparency, this polymer could and will be explored for potential application as a polymeric optically transparent electrode in display technologies. With the change in optical absorption as a function of changing the redox potential, this polymer may also find potential application in electrochromic displays or windows.

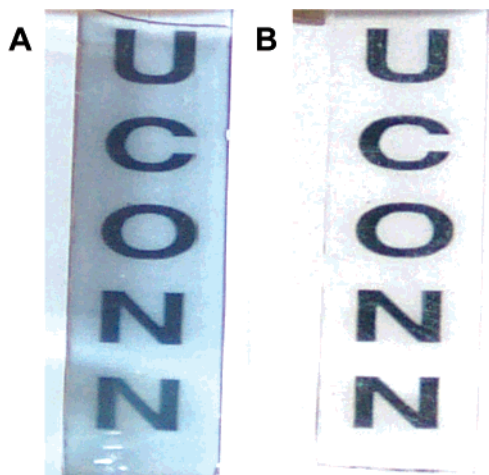


**Figure 6.** A 0.8  $\mu\text{m}$  thick poly(T34bT) film coated on an ITO-coated glass slide in the (A) reduced state at  $-0.8$  V and in the (B) oxidized semiconducting state at  $0.4$  V vs  $\text{Ag}/\text{Ag}^+$  reference electrode ( $0.47$  V vs NHE). The counter electrode was a platinum plate.

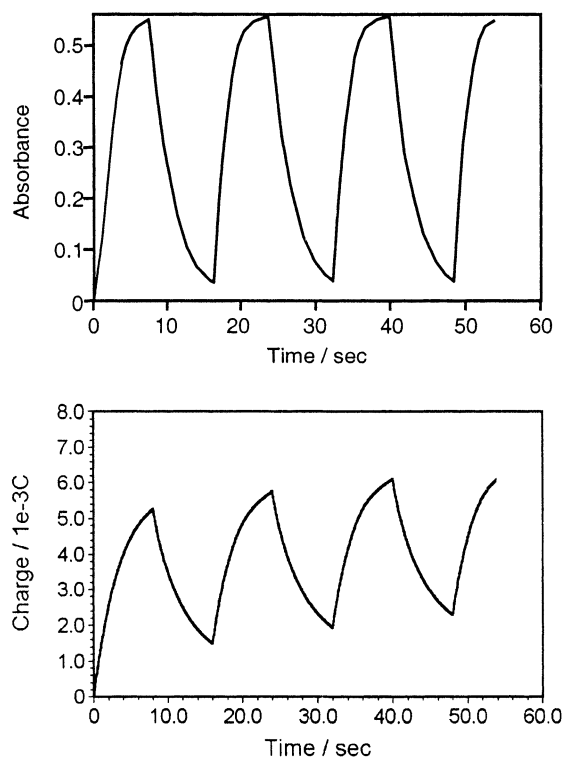


**Figure 7.** Chronoabsorptometry (A) and chronocoulometry (B) obtained for redox switching poly(T34bT) between  $-0.8$  and  $0.15$  V in  $0.1$  M lithium triflate/acetonitrile with a pulse width of  $8$  s. Only the first three full double potential steps of a total 100 that were taken are shown.

**Redox Switching Behavior.** Figure 7 shows the redox switching of a  $0.12$   $\mu\text{m}$  thick poly(T34bT) film coated onto an ITO glass slide between the reduced and p-doped conducting state utilizing chronoabsorptometry (Figure 7a) and chronocoulometry (Figure 7b). For this experiment, the polymer was switched between  $-0.8$  and  $0.15$  V in  $0.1$  M lithium triflate/acetonitrile with a pulse length of  $8$  s. Therefore, it takes  $16$  s to complete a double potential step, the process of stepping to the oxidized state and back to the reduced state before switching to the oxidized state again. As shown in Figure 7, it takes approximately  $4$  s for the polymer to switch from the oxidized semiconducting state to the

neutral insulating state in which the polymer transitions from transparent and colorless to a semitransparent sky-blue (see Figure 6), whereas it takes approximately  $6$  s for the polymer to switch from the neutral state to the oxidized state. It is significant to note that thinner films have more rapid response times. For example, T34bT films prepared on either platinum or ITO glass of approximately  $0.05$   $\mu\text{m}$  thickness switch from the oxidized to neutral state in  $0.1$  s and from the neutral to oxidized state in  $0.2$  s. For the particular system shown in Figure 7, the polymer was able to retain 95% electroactivity and 96% change in optical density upon undertaking 100 double potential steps.

**Coloration Efficiency.** To probe the usefulness of poly(T34bT) as a material for use in electrochromic applications, a coloration efficiency (CE) must be calculated in order to make comparisons with electrochromic materials previously reported in the literature. CE in units of  $\text{cm}^2/\text{coulomb}$  (C) is obtained by determining the injected/ejected charge as a function of the electrode area which is expressed in terms of charge density ( $Q_d$ ) in units of  $\text{C}/\text{cm}^2$  and through the determination of the change in optical density ( $\Delta\text{OD}$ ) which is obtained from the chronoabsorptometry and chronocoulometry data acquired from a redox step of the polymer.  $\Delta\text{OD}$  at a specified wavelength is expressed as

$$\Delta\text{OD}(\lambda) = \log[T_b(\lambda)/T_c(\lambda)]$$

where  $T_b$  and  $T_c$  are the transmittance in the bleached and colored states, respectively. The CE at the same specified wavelength can be expressed as

$$\text{CE}(\lambda) = \Delta\text{OD}(\lambda)/Q_d$$

From the data shown in Figure 8 for a poly(T34bT) film with a surface area of  $1.4$   $\text{cm}^2$  and the values calculated for  $T_b$ ,  $T_c$ , and  $Q_d$  being  $0.955$ ,  $0.295$ , and  $0.0032$   $\text{C}/\text{cm}^2$ , respectively, the CE for poly(T34bT) is calculated to be  $160$   $\text{cm}^2/\text{C}$  at a wavelength of  $800$  nm.

For amorphous tungsten trioxide ( $\text{WO}_3$ ) films prepared via thermal evaporation, the CE was  $115$   $\text{cm}^2/\text{C}$  ( $633$  nm), whereas  $\text{WO}_3$  prepared in polycrystalline morphologies via sputtering of lead give reported CE values of approximately  $50$   $\text{cm}^2/\text{C}$ .<sup>23</sup> The most widely investigated anodically coloring metal oxide is iridium dioxide ( $\text{IrO}_2$ ), which exhibits a color change from transparent and colorless to blue-black and has CE values ranging from  $15$  to  $20$   $\text{cm}^2/\text{C}$ .<sup>24</sup> Conducting polymers exhibit higher CE values due to lower power requirements. The porous morphologies of these coatings facilitate diffusion of counterions during the oxidation and reduction process. Typically, polythiophenes have CE values ranging from  $100$  to  $300$   $\text{cm}^2/\text{C}$ .<sup>25</sup> Although poly(T34bT) exhibits a CE in midrange with respect to other conventional polythiophenes, the advantage that this system has is that in the oxidized state the polymer is colorless as opposed to most previously reported conductive polymer systems which exhibit a noticeable color in both the reduced and oxidized states. Poly(T34bT) would be ideal as a cathodically coloring polymer for incorporation into dual polymer electrochromics that have been previously reported.<sup>26</sup>

## Conclusion

Herein, we have described the preparation and characterization of a new stable low band gap polymer

consisting of thieno[3,4-*b*]thiophene. T34bT has an oxidation potential between that of pyrrole and 3,4-ethylenedioxythiophene, making it a low oxidation monomer. The polymer prepared from T34bT has a low band gap and, as such, can be both easily oxidized and easily reduced to form doped polymer. We have found that poly(T34bT) is highly stable to redox switching between the p-doped and neutral forms and is stable upon cycling completely through both the p- and n-doped states. Poly-(T34bT) is sky-blue in the reduced form and both colorless and highly transparent in the oxidized, semiconductive state. Thus, with these properties this polymer could serve in applications such as coatings for electrochromic displays/devices or as coatings for use as optically transparent electrodes (OTE). Our future work will entail detailed dopant ion transport studies and the use of poly(T34bT) as an optically transparent electrode.

**Acknowledgment.** We thank the University of Connecticut Research Foundation for financial support of this work.

## References and Notes

- (1) (a) Chiang, C. K.; Fincher, C. R., Jr.; Park, Y. W.; Heeger, A. J.; Shirakawa, H.; Louis, E. J.; Gau, S. C.; MacDiarmid, A. G. *Phys. Rev. Lett.* **1977**, *39*, 1098. (b) Shirakawa, H.; Louis, E. J.; MacDiarmid, A. G.; Chiang, C. K.; Heeger, A. J. *J. Chem. Soc., Chem. Commun.* **1977**, 578.
- (2) Jonas, F.; Heywang, G. *Electrochim. Acta* **1994**, *39*, 1345.
- (3) Yu, G.; Heeger, A. J. *Synth. Met.* **1997**, *85*, 1183.
- (4) (a) Schwendeman, I.; Hwang, J.; Welsh, D. M.; Tanner, D. B.; Reynolds, J. R. *Adv. Mater.* **2001**, *13*, 634. (b) Schottland, P.; Zong, K.; Gaupp, C. L.; Thompson, B. C.; Thomas, C. A.; Giurgiu, I.; Hickman, R.; Abboud, K. A.; Reynolds, J. R. *Macromolecules* **2000**, *33*, 7051. (c) Thompson, B. C.; Schottland, P.; Zong, K.; Reynolds, J. R. *Chem. Mater.* **2000**, *12*, 1563.
- (5) (a) McQuade, D. T.; Pullen, A. E.; Swager, T. M. *Chem. Rev.* **2000**, *100*, 2537. (b) Yang, J.-S.; Swager, T. M. *J. Am. Chem. Soc.* **1998**, *120*, 11864. (c) Sotzing, G. A.; Briglin, S.; Grubbs, R. H.; Lewis, N. S. *Anal. Chem.* **2000**, *72*, 3181.
- (6) (a) Tour, J. M. *Polym. News* **2000**, *25*, 329. (b) Tour, J. M. *Acc. Chem. Res.* **2000**, *33*, 791.
- (7) (a) Heywang, G.; Jonas, F. *Adv. Mater.* **1992**, *4*, 116. (b) Groenendaal, B.; Jonas, F.; Freitag, D.; Pielartzik, H.; Reynolds, J. *Adv. Mater.* **2000**, *12*, 481.
- (8) (a) Dietrich, M.; Heinze, J.; Heywang, G.; Jonas, F. *J. Electroanal. Chem.* **1994**, *369*, 87. (b) Sotzing, G.; Reynolds, J.; Steel, P. *Adv. Mater.* **1997**, *9*, 795.
- (9) Jonas, F.; Krafft, W. US Patent 5,300,575, 1994.
- (10) (a) Kim, J. Y.; Jung, J. H.; Lee, D. E.; Joo, J. *Synth. Met.* **2002**, *126*, 311. (b) Ahonen, H. J.; Lukkari, J.; Kankare, J. *Macromolecules* **2000**, *33*, 6787.
- (11) Pei, Q.; Zuccarello, G.; Ahlsgog, M.; Inganas, O. *Polymer* **1994**, *35*, 1347.
- (12) (a) Roncali, J. *Chem. Rev.* **1997**, *97*, 173. (b) Pomerantz, M. In *Handbook of Conducting Polymers*, 2nd ed.; Skotheim, T. A., Elsenbaumer, R. L., Reynolds, J. R., Eds.; Marcel Dekker: New York, 1998; Chapter 11, pp 277–311.
- (13) (a) Kobayashi, M.; Colaneri, N.; Boysel, M.; Wudl, F.; Heeger, A. J. *J. Chem. Phys.* **1985**, *82*, 5717. (b) Colaneri, N.; Kobayashi, M.; Heeger, A. J.; Wudl, F. *Synth. Met.* **1986**, *14*, 45. (c) Wudl, F.; Kobayashi, M.; Heeger, A. J. *J. Org. Chem.* **1984**, *49*, 3382.
- (14) Lee, K.; Sotzing, G. *Macromolecules* **2001**, *34*, 5746.
- (15) (a) Lawesson, S. *Ark. Kemi* **1957**, *11*, 325. (b) Janda, M.; Srogl, J.; Stibor, I.; Nemec, M.; Vopatrna, P. *Synthesis* **1972**, *10*, 545.
- (16) Watson, S. C.; Eastman, J. F. *J. Organomet. Chem.* **1967**, *9*, 165.
- (17) Brandsma, L.; Verkruijsse, H. D. *Synth. Commun.* **1990**, *20*, 2275.
- (18) Wynberg, H.; Feijen, J. *Recueil* **1970**, *89*, 77.
- (19) Wynberg, H. *Tetrahedron Lett.* **1967**, *9*, 761.
- (20) T. A.; Elsenbaumer, R. L., Reynolds, J. R., Eds.; *Handbook of Conducting Polymers*, 2nd ed.; Skotheim, Marcel Dekker: New York, 1998.
- (21) Semenikhin, O. A.; Ovsyannikova, E. V.; Ehrenburg, M. R.; Alpatova, N. M.; Kazarinov, V. E. *J. Electroanal. Chem.* **2000**, *494*, 1.
- (22) Hong, S. Y.; Marynick, D. S. *Macromolecules* **1992**, *25*, 4652.
- (23) (a) Faugnan, B. W.; Crandall, R. S.; Heyman, P. M. *RCA Rev.* **1975**, *36*, 177. (b) Hitchman, M. J. *J. Electroanal. Chem.* **1977**, *85*, 135.
- (24) Dautremont-Smith, W. C. *Displays I* **1982**, *3*.
- (25) Mastragostino, M.; Arbizzani, C.; Ferloni, P.; Marinangeli, A. *Solid State Ionics* **1992**, *53–56*, 471.
- (26) (a) Sapp, S. A.; Sotzing, G. A.; Reynolds, J. R. *Chem. Mater.* **1998**, *10*, 2101. (b) De Paolia, M.-A.; Casalbore-Miceli, G.; Girotto, E. M.; Gazotti, W. A. *Electrochim. Acta* **1999**, *44*, 2983.

MA020367J